MUSCLE INERTIA DURING RUNNING: A MASSIVE CHANGE OF MOMENTS?

Jasper Verheul[1,2], Shinjiro Sueda[3], Sang-Hoon Yeo[2]

[1]School of Sport and Health Sciences, Cardiff Metropolitan University, Cardiff, UK
[2]School of Sport, Exercise & Rehabilitation Sciences, University of Birmingham, Birmingham, UK
[3]Department of Computer Science and Engineering, Texas A&M University, TX, US

Skeletal muscles have substantial inertia that cause inertial forces working around joints. These inertial forces are not typically considered in musculoskeletal models used for sport biomechanics research, which can lead to considerable errors in estimated joint kinetics. How large these errors are in common sports movements is yet unclear. We therefore examined the role of shank muscle inertia on ankle joint moments during the swing phase of running at different speeds. Ankle moments were considerably affected when muscles were modelled as separate masses, with a general shift towards reduced dorsiflexion and higher plantarflexion moments. These results show that ignoring inertial muscle forces in musculoskeletal simulations can lead to under- or overestimations of structure-specific loads and possibly erroneous conclusions. We therefore encourage sport biomechanics researchers to consider the impact of muscle inertia on inverse dynamics calculations.

KEYWORDS: muscle inertia, running mechanics, musculoskeletal modelling.

INTRODUCTION: Musculoskeletal simulations of sports movements allow for quantifying kinetic variables that are difficult to measure *in vivo*. Inverse dynamics results depend on the mass and inertial properties of the segments included in a model (Rao et al., 2006). These segment properties are typically taken from cadaver or MRI measurements and combine the mass of muscles, tendons, bones, cartilage, and connective tissues. This approach is convenient but has a major limitation. Since muscles are connected to multiple segments, muscle mass directly affects the effective inertia of the joints they act around. Hence, joint inertia is likely to be over- or underestimated by combining muscle masses with their nearest segment, leading to incorrect predictions of the dynamics of musculoskeletal systems. Simple theoretical examples have indeed shown that combining muscles in the total segmental mass can cause substantial errors in joint kinetics, and that errors are nonuniform and dependent on joint orientation and velocity (Pai, 2010). Nevertheless, it is yet unclear how these findings translate to simulations of common sports movements.

Running is a popular and arguably the most widely studied sport. Human running is characterised by the absence of a double support phase and a distinct stance and swing phase (Novacheck, 1998). Since no considerable external forces (e.g., ground reaction forces) act on the leg during the swing phase, joint kinetics are mainly determined by gravity and inertia. This allows for isolating the effects of inertial-property changes on individual joint kinetics. Moreover, substantial increases in joint range of motion and segmental velocities at higher running speeds make it likely that inertial-property effects can be further highlighted when running faster. This makes running, and the swing phase in particular, a suitable movement for investigating the effects of muscle inertia on joint kinetics.

The tibialis anterior is the primary dorsiflexor of the ankle joint. Increased ankle dorsiflexion moments due to calf muscle inertia can thus reasonably be assumed to roughly translate to increased tibialis anterior force demands. This makes the ankle an ideal joint to estimate how muscle inertia might impact the force requirements of an individual muscle. In this study we therefore examined the effect of shank-muscle inertia on ankle kinetics during the swing phase of running. We hypothesised that 1) dorsiflexion moments are higher when muscle mass is modelled separate from the shank, and that 2) differences in joint kinetics due to muscle inertia are more pronounced at higher running speeds.

METHODS: One healthy football player (male, 19 yrs, 185 cm, 76.3 kg) performed running trials on a motorised treadmill (Woodway Pro, Woodway UK). After a short warmup, treadmill familiarisation, and a static calibration trial, the participant performed two consecutive running trials at 10, 13, 17, and 19.1 km·h⁻¹. During the running trials, three-dimensional trajectories of 38 retro-reflective markers attached to the lower limbs and pelvis were recorded for ten seconds with eight infrared cameras (Qqus 300+, Qualisys) sampling at 250 Hz. Marker trajectories were filtered with a 4th-order Butterworth filter at 15 Hz and exported to OpenSim (v.4.3). The static calibration trials were used to scale the gait2392 model (Delp et al., 1990) to the participant's dimensions. Lower-limb kinematics were then calculated using inverse kinematics and exported to MATLAB (v.R2021a, MathWorks) for further processing and analysis.

Lower-limb kinematics and segmental properties (i.e., mass, centre of mass position, inertia) of the gait2392 model were used as input to RedMax – a custom MATLAB-based musculoskeletal simulator (Wang et al., 2019; Xu et al., 2021). RedMax was used to perform inverse dynamics, either with shank muscle masses included in the combined shank mass (CSM) or modelled as separate muscle masses (SMM). For SMM, the total mass of the shank segment (3.76 kg) was divided between four muscles: tibialis anterior (12.1%; 0.45 kg), soleus (41.5%; 1.56 kg), gastrocnemius medialis (17.1%; 0.64 kg) and lateralis (9.4% 0.35 kg), and the tibia bone plus remaining muscles and connective tissues (20%; 0.75 kg), based on mean cadaver data (Ward et al., 2009). Muscle insertion points on the thigh, shank and foot segments, as well as muscle wrapping surfaces and via points, were as defined by Rajagopal et al. (2016) (Figure 1). Twenty discrete mass points were distributed uniformly along the four muscle paths. Tendon lengths were divided into two equal lengths for the proximal and distal ends of the muscle-tendon unit, and muscle mass points distributed along the remaining length, considering wrapping surfaces and via points.
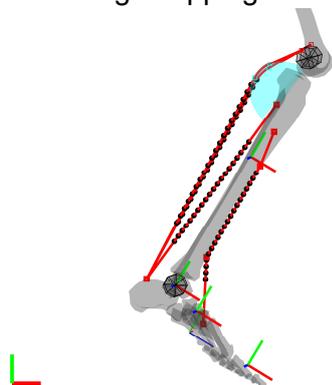
Figure 1: Discrete mass points (*n=20*) were distributed along the muscle paths of the tibialis anterior, soleus, and gastrocnemius medialis and lateralis. Local coordinate systems show the segmental centre of mass location.

Starting with the standard equations of motion for the r degrees of freedom of the skeletal joints, $M_s\ddot{q} = f_s$ (where M_s is the inertia, and f_s are the gravity and Coriolis forces of the skeleton), the generalized inertia and the generalized force were augmented as:

$$(M_s + J^T M_a J)\ddot{q} = f_s + J^T(f_a - M_a \dot{J}\dot{q})$$

in which M_a is the $3n \times 3n$ inertia tensor of the muscles with n being the total number of mass points ($n = 20$), f_a is the $3n \times 1$ force vector acting on the muscles due to gravity, and J is the $3n \times r$ Jacobian matrix to convert joint velocities to muscle mass velocities. The Jacobian and its time derivative were computed with a forward finite differencing scheme at each time step.

Individual swing phases of the right leg were cut from the ten-second trials between take off and initial contact, based on maximal knee extension angle (Fellin et al., 2010) and minimal vertical pelvis centre of mass velocity (Milner and Paquette, 2015) respectively. Mean root mean square errors (RMSE) between ankle moments simulated with CSM and SMM were calculated, together with differences in peak dorsiflexion and plantarflexion moments. A two-way repeated measures ANOVA (p=0.05) was performed for peak dorsiflexion and plantarflexion moments between CSM and SMM across the four running speeds.

RESULTS: Modelling the four major shank muscles as SMM had a considerable impact on the simulated ankle joint moments, with a general decrease and increase in dorsiflexion and plantarflexion moments respectively (Figure 2).
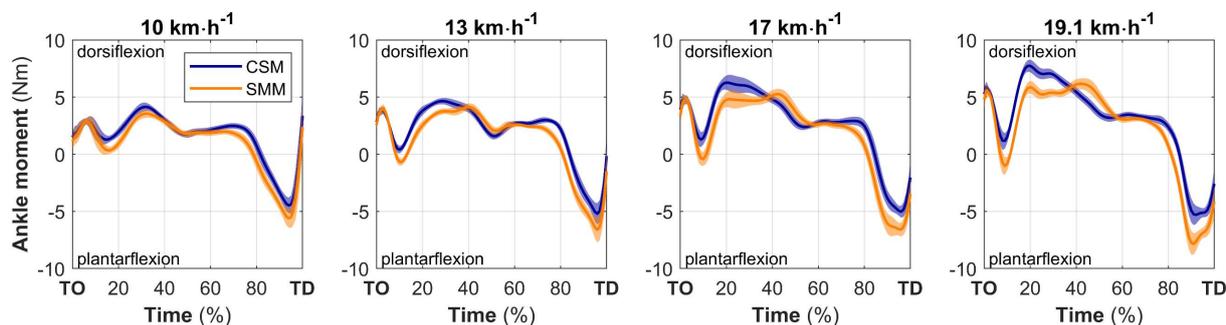
Figure 2: Ankle moment profiles (mean ± standard deviation) during the swing phase of running at four different speeds, simulated with either a combined shank mass (CSM; blue) or separate muscle masses (SMM; orange). *TO*: take off; *TD*: touch down.

Differences in peak moments between CSM and SMM (Table 1) ranged from 8-18% (dorsiflexion) and 24-42% (plantarflexion). There was a significant main effect ($p<0.001$) of muscle modelling condition and running speed, and a significant interaction between modelling condition and speed ($p<0.001$).

Table 1: Ankle moment comparison between CSM and SMM across the four running speeds

	Running speed			
	10 km·h^{-1}	13 km·h^{-1}	17 km·h^{-1}	19.1 km·h^{-1}
Swing phases (n)	24	24	27	27
Time-series RMSE (Nm)	0.8±0	1±0	1.3±0.1	1.6±0.1
Δ peak dorsiflexion moment (Nm)	0.7±0.3	0.4±0.3	0.9±0.3	1.4±0.3
Δ peak plantarflexion moment (Nm)	1.1±0.2	1.4±0.2	1.7±0.3	2.4±0.3

Values are mean ± standard deviation. RMSE = root mean square error; Δ = difference.

DISCUSSION: In this study we demonstrated that modelling shank muscles as separate masses substantially affects ankle kinetics during the swing phase of running. To the best of our knowledge, this is the first study to demonstrate muscle-inertia effects in a simulation of a common sports movement.

In contrast to our first hypothesis, we found a general decrease in dorsiflexion moments. A reason for this could be that centrifugal forces counter the inertial forces due to muscle lengthening. The major difference between this study and Pai (2010) was that their model did not move as a whole. In our simulation of running however, the whole leg moved throughout the swing phase, likely causing inertial centrifugal forces working towards the ankle (i.e., opposite to the contractile forces of the calf muscles). These centrifugal forces can thus lead to a decrease in required dorsiflexion moments and so offset the hypothesised increase. Furthermore, the centrifugal force due to calf-muscle inertia also explains the increase in required plantarflexion moments observed towards the end of the swing phase (Figure 1). Since the centrifugal force is proportional to the square of the angular velocity, one would expect centrifugal forces to increase because of higher leg-swing velocities at higher running speeds. Consistent with our second hypothesis, we did indeed find a more pronounced difference in ankle moments between CSM and SMM when running speed increased, which further supports the theory that different inertial forces can counter each other.

Since the tibialis anterior is the primary dorsiflexor of the ankle joint, changes in dorsiflexion moments can be reasonably assumed to affect tibialis anterior force requirements. Peak dorsiflexion moment reductions of up to 18% suggest that tibialis anterior force demands can be substantially overestimated when using CSM, which can have implications for investigations

of running-related injuries that are associated with tibialis anterior fatigue and overuse, such as chronic exertional compartment syndrome (Franklyn-Miller et al., 2014). However, the muscle inertia effects demonstrated in this simple example are likely to be further magnified in other scenarios, especially those including high-velocity movements, joints crossed by biarticular muscles, and/or large muscle masses. We therefore encourage sport biomechanics researchers to consider the role of muscle inertia when investigating other, more complex running-related injury mechanisms, such as the impact of inertial forces of the thigh muscles on hamstring force demands during the swing phase of high-velocity running (i.e., sprinting).

Our results reveal a substantial impact of muscle inertia on joint kinetics during running. Hence, an important question is how muscle inertia should be accounted for in musculoskeletal models used for sport biomechanics research. Several options have been suggested by Pai (2010): not changing anything, adding mass to existing muscle models (e.g., Ross and Wakeling (2016)), calculating each muscle's contribution to joint inertia (as in this study), or using continuum-mechanics based muscle models (e.g., finite element models). Each of these solutions comes with its own benefits and disadvantages that should be carefully weighed. Perhaps the main consideration is that most sport biomechanics researchers and practitioners rely on existing models from openly available musculoskeletal simulation software (e.g., OpenSim, Visual3D). Widespread consideration of the impact of muscle inertia in sport biomechanics research is therefore likely dependent on future implementations of mass properties in commonly used phenomenological muscle models (i.e., Hill-type models (Zajac, 1989)) or of each muscle's contribution to the joint inertia within existing simulators.

CONCLUSION: This study demonstrates that ignoring muscle inertia has a considerable impact on the predicted ankle moments during the swing phase of running. Since over- or underestimations of structure-specific loads experienced during sports can lead to erroneous conclusions, we encourage sport biomechanics researchers to carefully consider the role of muscle inertia in inverse dynamics calculations for sports movements.

REFERENCES

Delp, S.L., Loan, J.P., Hoy, M.G., Zajac, F.E., Topp, E.L., Rosen, J.M., 1990. An Interactive Graphics-Based Model of the Lower Extremity to Study Orthopaedic Surgical Procedures. IEEE Trans. Biomed. Eng.

Fellin, R.E., Rose, W.C., Royer, T.D., Davis, I.S., 2010. Comparison of methods for kinematic identification of footstrike and toe-off during overground and treadmill running. J. Sci. Med. Sport 13, 646–650.

Franklyn-Miller, A., Roberts, A., Hulse, D., Foster, J., 2014. Biomechanical overload syndrome: Defining a new diagnosis. Br. J. Sports Med. 48, 415–416.

Milner, C.E., Paquette, M.R., 2015. A kinematic method to detect foot contact during running for all foot strike patterns. J. Biomech. 48, 3502–3505.

Novacheck, T.F., 1998. The biomechanics of running. Gait Posture 7, 77–95.

Pai, D.K., 2010. Muscle mass in musculoskeletal models. J. Biomech. 43, 2093–2098.

Rajagopal, A., Dembia, C.L., DeMers, M.S., Delp, D.D., Hicks, J.L., Delp, S.L., 2016. Full-Body Musculoskeletal Model for Muscle-Driven Simulation of Human Gait. IEEE Trans. Biomed. Eng. 63, 2068–2079.

Rao, G., Amarantini, D., Berton, E., Favier, D., 2006. Influence of body segments' parameters estimation models on inverse dynamics solutions during gait. J. Biomech. 39, 1531–1536.

Ross, S.A., Wakeling, J.M., 2016. Muscle shortening velocity depends on tissue inertia and level of activation during submaximal contractions. Biol. Lett. 12, 10–13.

Wang, Y., Weidner, N.J., Baxter, M.A., Hwang, Y., Kaufman, D.M., Sueda, S., 2019. RedMax: Efficient & flexible approach for articulated dynamics. ACM Trans. Graph. 38, 104.

Ward, S.R., Eng, C.M., Smallwood, L.H., Lieber, R.L., 2009. Are current measurements of lower extremity muscle architecture accurate? Clin. Orthop. Relat. Res. 467, 1074–1082.

Xu, J., Chen, T., Zlokapa, L., Foshey, M., Matusik, W., Sueda, S., Agrawal, P., 2021. An End-to-End Differentiable Framework for Contact-Aware Robot Design. Proc. Robot. Sci. Syst.

Zajac, F.E., 1989. Muscle and tendon: properties, models, scaling, and application to biomechanics and motor control. Crit. Rev. Biomed. Eng. 17, 359–411.